Preparing tokamak 3D wall and magnetic data
for particle tracing simulations

S. Äkäslompolo[1], T. Koskela[1], T. Kurki-Suonio[1], T. Lunt[2], J. Miettunen[1], E. Hirvijoki[1],

The ASDEX Upgrade Team[2], ITM-TF contributors[*]

[1] *Aalto University, Espoo, Finland*

[2] *Max-Planck-Institut für Plasmaphysik, Garching, Germany*

A real tokamak has non-axisymmetric first wall and magnetic field. Detailed simulations, e.g. of fast ions, are affected by the toroidal asymmetry. This contribution describes methods related to reducing the full CAD data to a simplified 3D first wall description and to computing the 3D-error field from arbitrary coil geometry or ferritic material distribution.

Magnetic field from coils with Biot-Savart law and magnetizing materials with FEM
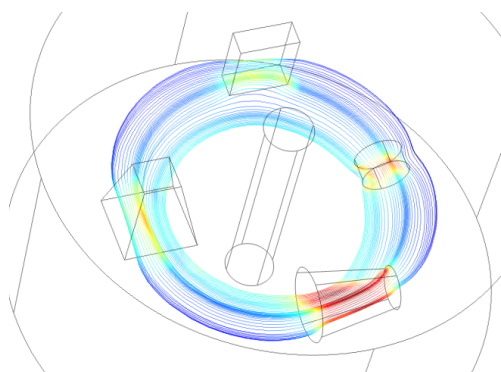

Figure 1: A toroidal $\sim 1/R$ field magnetizes four geometrical solid ferromagnetic bodies. The color coded line is a single field line, with color indicating the local field strength. The cylinder in the middle excludes the singular area with $R = 0$ from the computational domain (a pierced cylinder).

In ITER, ferritic inserts will be used to reduce the magnetic ripple due to the finite number of toroidal field coils. Furthermore, the tritium breeding modules (TBM) will be made out of ferromagnetic steel. The toroidal and poloidal distributions of these magnetizing masses are irregular and induce a perturbation to the magnetic field in ITER[1]. We use the commercial *COMSOL Multiphysics* engineering, design, and finite element method (FEM) analysis software environment to calculate the magnetization of the ferromagnetic components according to the equations $\nabla \times \vec{H} = \vec{J}_e = 0$, $\vec{B} = \nabla \times \left(\vec{A} + \vec{A}_b \right)$ and $\vec{B} = \mu_0 \mu_r \vec{H}$. The background vector potential $\vec{A}_b$ is calculated from the plasma and coil as described later in this contribution. The boundary condition is vanishing field from the magnetization when far away from the machine. A result from a toy model is illustrated by the Fig. 1.

The $B(H)$ curve models the magnetic properties of a nonlinear material (e.g. saturating ferromagnetic metal) in COMSOL. Here B is the magnetic flux density produced by the magnetizing field H. A set of minimal material parameters to reproduce the key features of the curve are the

following three: the saturation magnetization M_s, remnant magnetisation M_r, and the coercive field H_c. With these, one can produce a piecewise linear model, where the magnetization is linear until saturation is achieved and beyond that increases at the rate of vacuum magnetization μ_0.

This approach neglects the detailed form of the $B(H)$ curve, as well as any contributions of the material beyond saturation. The error from the former approximation is expected to dominate, since the saturation field H_s can only be calculated using differential permeability $\mu^d(H) \equiv \frac{\partial B(H)}{\partial H}$ at low fields: $\mu^d(H < H_s) = M_r/H_c$. Therefore, the saturation field $H_s = \frac{M_s - M_r}{\mu^d(H<H_s)}$ is calculated using low field values (Fig. 2). The latter error is expected to be small: $\mu^d(H > H_s)/\mu_0 \approx 1.001$.

The vacuum magnetic field $\vec{B}$ and the magnetic vector potential $\vec{A}$ is calculated with the recent *Bio-Saw* <u>Bio</u>t–<u>S</u>avart <u>law</u>* integrator from the coil currents or plasma current, by assuming a thin conductor $\vec{R}(s)$: $\vec{B}(\vec{r}) = \frac{\mu_0}{4\pi} I \int \frac{\hat{\ell}(s) \times (\vec{r} - \vec{R}(s))}{|\vec{r} - \vec{R}(s)|^3} ds$ and $\vec{A}(\vec{r}) = \frac{\mu_0}{4\pi} I \int \frac{\hat{\ell}(s)}{|\vec{r} - \vec{R}(s)|} ds$ [2], where s depict distance along the coil, $\hat{\ell}(s)$ is a unit vector along $\vec{R}(s)$ and I the

Figure 2: Three point model for magnetization curve. The simplified model approximately reproduces the original B(H) curve. Notice how the simple model changes H_s.

current. The coil geometry is approximated with a spline (independently in each dimension) and then numerically integrated [3] over the coil (along s) in each evaluation point $\vec{r}$ independently.

In addition to the vacuum field, also the plasma current produces a significant magnetic field. If the current can be assumed toroidally symmetric, the field or vector potential can be acquired quickly by evaluating directly the well known field due to a current loop [4, 5]. For the involved elliptical integrals we exploit the *SLATEC* library [6].

3D-first wall from CAD data with ray-tracing and smoothing

The task is to extract the plasma facing components from an unordered and potentially large CAD drawing database into a format useful for plasma physics codes. This is done by first exporting the drawings to a simpler format, then extracting the plasma facing components by ray-tracing and finally reducing the dataset in to the essential information. The procedure was
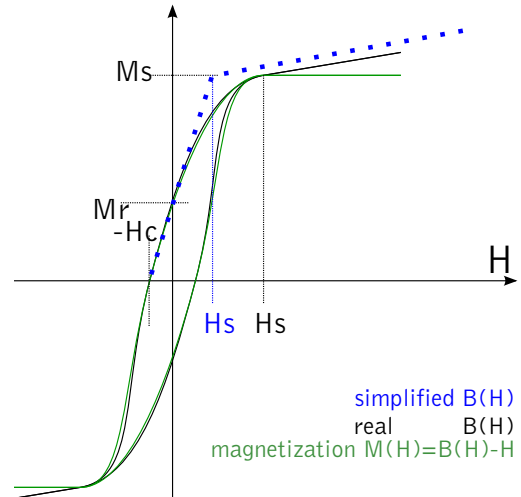
---

*See also T. Koskela *et al.* (O4.109 in these proceedings) for employing of BioSaw for ITER ELM coils.

developed within an EFDA Integrated Tokamak Modelling Task Force[†] project. The following is a more detailed description of the method.
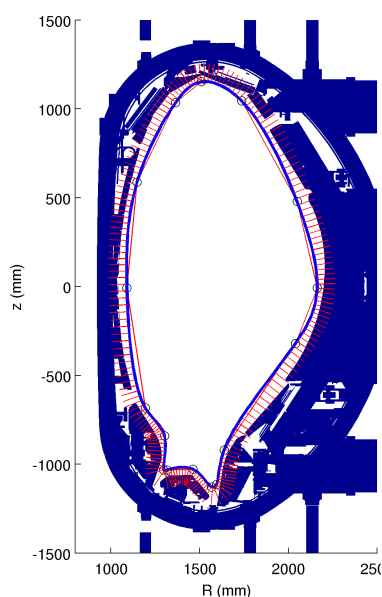

Figure 3: The method to produce the line family: The red broken-line is manually drawn. The blue curve is a spline fit with the red lines showing the ray directions.

The CAD drawings of all in-vessel components are exported into a simple list of triangles in 3D-space. To select the rays for the ray-tracing, a family of radial lines in a poloidal plane pointing from the plasma to the wall is chosen such that the entire poloidal cross section is covered. The process to create the radial line family is illustrated by Fig. 3. The first step is to manually draw such a guiding curve, that closely follows the poloidal projection of the first wall, but is slightly offset towards the plasma. A spline is then fit to this curve. The family of radial lines is then formed by evaluating the normals of the guiding spline. The lines are toroidally duplicated to form an arbitrarily dense rectangular grid in toroidal-poloidal space and used as the rays. Originally ellipses were used instead of arbitrary curves, but later more flexibility is required for wider applicability.

Each line is then ray-traced to pinpoint the nearest-to-the-plasma intersection with the wall. The intersection points now describe the first wall with the requisite precision and constitute a dense rectangular grid in toroidal-poloidal space. Unfortunately, the grid contains anomalies due to numerical errors and excessive details, such as screw holes, and hence needs further processing. A smoothing spline is fitted to this 2D grid, where the ordinate is the distance from the curve to the intersection. For different parameters of the smoothing spline fitting, different levels of details can be sustained, as is illustrated by Fig. 4. Since the defeaturing removes most of the fine details, the final wall mesh can be significantly smaller than the original dense grid. The guiding spline and smoothing 2D-spline can be evaluated at arbitrary locations to produce the final grid at arbitrary mesh size. The final wall is compared against the original CAD data in Fig. 5.

Applications

In ref [7, 8] it was shown that the 3D features of the wall can have a dramatic effect on the particle deposition patterns in test particle simulations. Recently the JET wall was produced and
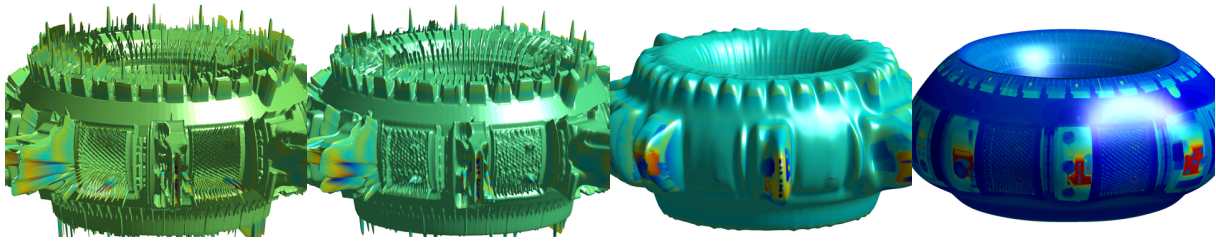
[†]http://www.efda-itm.eu/

Figure 4: The AUG wall defeatured with the smoothing strengthening from left to right.

the first results [9] show the importance of 3D features also in JET. The next step is to create a similar wall describing the ITER tokamak, as well as produce a 3D-magnetic background including the EU tritium breeding test blanket module. The first use for the ITER data will be calculation of fast ion behaviour.

References

[1] K. Shinohara *et al.* Fusion Eng. Des., **84** 1 (2009)

[2] J. Vanderlinde, Classical Electromagetic Theory, 2nd ed. page 23

[3] R Piessens *et al.* QUADPACK: A Subroutine Package for Automatic Integration

[4] Albert Shadowitz. The Electromagnetic Field. Dover Publications, Inc., New York, 1975.

[5] Kevin Kuns, Calculation of Magnetic Field Inside Plasma Chamber `http://plasmalab.pbwiki.com/f/bfield.pdf`

[6] SLATEC Common Mathematical Library, `http://www.netlib.org/slatec/`

[7] J. Miettunen *et al.* Nucl. Fusion **52** 032001 (2012)

[8] Asunta *et al.* in press Nucl. Fusion (2012)

[9] J. Miettunen *et al.* 20th Internat. Conf. on Plasma Surface Interactions 2012 P1-090
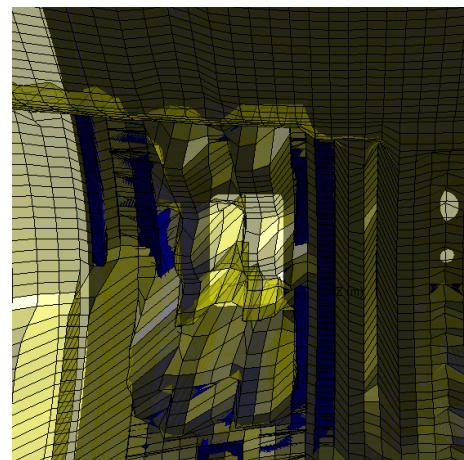
Figure 5: A detail from a comparison of the triangle data from the CAD and defeatured wall mesh. The blue triangles of the raw data partly penetrate the yellow translucent wall that roughly corresponds to leftmost panel in Fig. 4.